



**HAL**  
open science

## Experimental Thermal-Hydraulic Study Of A Steam-Droplets Flow Inside A Vertical Pipe -Application To Loca In PWR Reactor

Juan David Pena Carrillo, A. V. S. Oliveira, T Glantz, Michel Gradeck,  
Alexandre Labergue

► **To cite this version:**

Juan David Pena Carrillo, A. V. S. Oliveira, T Glantz, Michel Gradeck, Alexandre Labergue. Experimental Thermal-Hydraulic Study Of A Steam-Droplets Flow Inside A Vertical Pipe -Application To Loca In PWR Reactor. NURETH 18, Aug 2019, Portland (Oregon), United States. hal-02433923

**HAL Id: hal-02433923**

**<https://hal.science/hal-02433923>**

Submitted on 9 Jan 2020

**HAL** is a multi-disciplinary open access archive for the deposit and dissemination of scientific research documents, whether they are published or not. The documents may come from teaching and research institutions in France or abroad, or from public or private research centers.

L'archive ouverte pluridisciplinaire **HAL**, est destinée au dépôt et à la diffusion de documents scientifiques de niveau recherche, publiés ou non, émanant des établissements d'enseignement et de recherche français ou étrangers, des laboratoires publics ou privés.

# **EXPERIMENTAL THERMAL-HYDRAULIC STUDY OF A STEAM-DROPLETS FLOW INSIDE A VERTICAL PIPE – APPLICATION TO LOCA IN PWR REACTOR**

**J.D. Peña Carrillo, A.V.S. Oliveira, and T. Glantz**

Institut de Radioprotection et de Sureté Nucléaire, IRSN

Cadarache, Saint Paul lez Durance, France

juan-david.penacarrillo@irsn.fr; arthur.vieiradasilvaoliveira@irsn.fr; tony.glantz@irsn.fr

**M. Gradeck, A. Labergue**

LEMETA, UMR CNRS 7563

Université de Lorraine

2 avenue de la forêt de Haye, 54505, Vandoeuvre les Nancy, France

michel.gradeck@univ-lorraine.fr; alexandre.labergue@univ-lorraine.fr

## **ABSTRACT**

During a Loss of Coolant Accident (LOCA) in a Pressurized Water Reactor (PWR), partial or even complete drying of fuel assemblies may occur. In these conditions, the fuel temperature can increase leading to significant deformation of the fuel rod cladding and a partial blockage of the fluid domain. These zones can thus affect the cooling of the nuclear core during the reflooding phase by the emergency core cooling systems (ECCS). Investigating the cooling capacity as well as the thermal-hydraulic characteristics of the flow in these zones is a crucial point to guarantee nuclear safety. In order to characterize the cooling capacity of these deformed zones by a two-phase flow, an experimental set-up at sub-channel scale has been developed. The experimental set-up consists of a tubular Venturi test section, a droplet supply system and a superheated steam supply system. The test section is heated up to about 700°C before starting the flow composed of superheated steam and dispersed droplets. During the cooling phase, optical measurements are carried out upstream and downstream the test section to measure the droplets diameter, velocity and temperature, while an IR camera records the transient of the tube temperature. This paper presents experimental results with three different test section diameters to analyze the influence of the blockage ratio on the cooling capacity. The droplets evaporation was evident with their reduction in size downstream the heated tube.

## **KEYWORDS**

LOCA, Thermo-hydraulics, Infrared thermography, Phase-Doppler Analyzer, LIF thermography

## **1. INTRODUCTION**

One known accidental condition that a Pressurized Water Reactor (PWR) can go through is the Loss Of Coolant Accident, usually referred to as LOCA. This might take place if a break occurs in the primary circuit or a sealing fails, leading to a dry-out of the nuclear core. By consequence, the heat dissipation of the fuel rods is no longer effective and their temperature increases substantially. Then, emergency core cooling systems (ECCS) are suddenly activated to control this temperature increase and, afterward, cool down the fuel rods. This process is known as the reflooding and it consists of injecting water to submerge the fuel rods. However, during this phase, water evaporates when in contact with the fuel claddings at

very high temperatures (up to 1200 °C) and creates a two-phase flow of steam and droplets downstream the quenching front [1, 2]. We can see in Figure 1 an illustrative curve of the process that undergoes during a LOCA. Therefore, during the first period of the reflooding phase, the upper part of the fuel rods is cooled down by this mist flow, so understanding this cooling process is important to evaluate the safety condition of a PWR during a hypothetical LOCA.

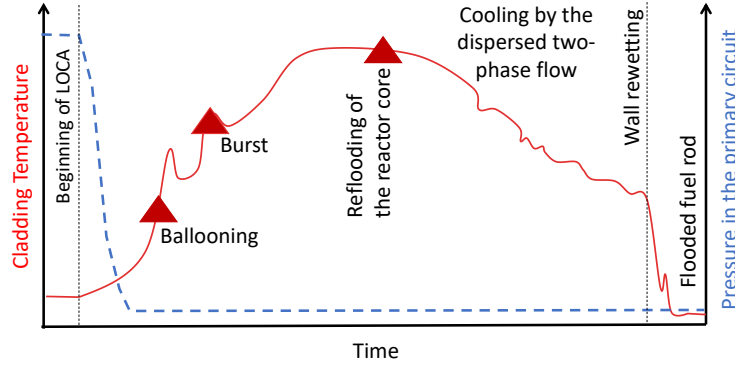


**Figure 1. Evolution of LOCA after a large break in the primary circuit.**

As shown in Figure 1, at a given moment during the heating of the fuel rods, the fuel claddings start to deform (“ballooning”). If the temperature continues to increase, the claddings no longer withstand the internal pressure and they burst, creating deformed or even blocked sub-channels that decrease the cross-sectional area of the flow passage. Hence, the cooling process of these regions might be affected and endanger the nuclear core structure.

To guarantee nuclear safety, numerical simulation tools, like IRSN’s DRACCAR code [3, 4], and mechanistic models [5–7] try to predict the heating and cooling of fuel rods in LOCA conditions. However, experimental data are still necessary to validate these calculations, especially at particular conditions, like with different blockage ratios caused by the ballooning of claddings. Thus, we built an experimental bench to perform tests at sub-channel scale of the cooling process in LOCA conditions, which consists of a vertical pipe with an internal flow of steam and droplets. In this work, we present results regarding the effect of the blockage ratio on the cooling process and on the internal flow characteristics.

## 2. EXPERIMENTAL APPARATUS AND TEST METHODOLOGY

The experimental bench, named COLIBRI (**COoL**ing of **B**lockage **R**egion **I**nside a PWR **R**eactor) is the same used in a previous work [8] and is presented in Figure 2. This apparatus consists basically of a droplet injection system, overheated steam injection system and an assembly of vertical tubes as test section.

The tubular assembly is divided into three parts, all made of Inconel 325: Part I and III are fixed and have an internal diameter of 11.78 mm, representing a not-deformed sub-channel of a typical PWR nuclear core. Part II is heated by Joule effect by using a DC-current power supply and is removable to place the test section with the desired geometry. In this study, we used three configurations as we present in Table I. Configuration 1 stands for the referential condition with no deformation, while the other two represent a 61% and a 90% blockage ratio  $\tau_b$ , which is defined by the following expression:

$$\tau_b = 1 - \frac{S_t}{S_0} \quad (1)$$

where  $S_t$  is the restriction cross-section area (with diameter  $D_h$ ), and  $S_0$  is the cross-sectional area of the tube with 11.78 mm diameter (not deformed).

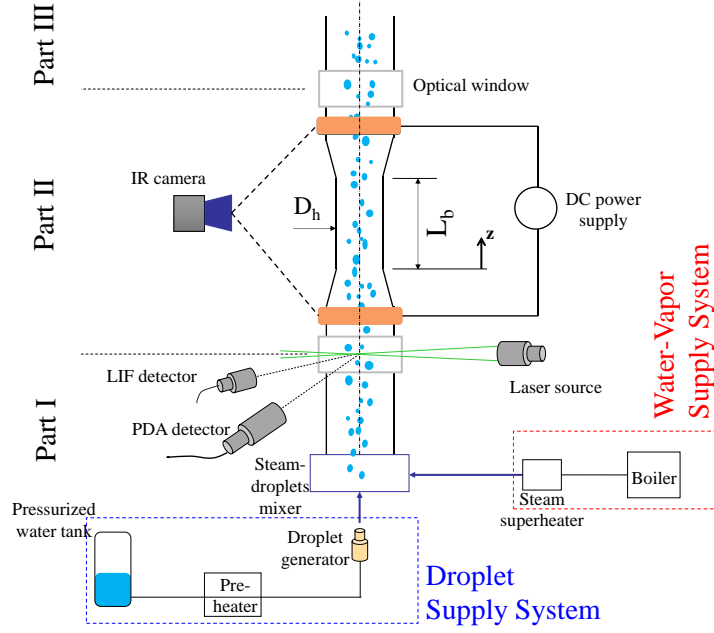


Figure 2. Schematic drawing of the COLIBRI experimental apparatus.

Table I. Geometrical characteristics of Part II

	<i>Configuration 1</i>	<i>Configuration 2</i>	<i>Configuration 3</i>
Blockage ratio ( $\tau_b$ )	0%	61%	90%
Hydraulic diameter ( $D_h$ )	11.78 mm	7.35 mm	3.72 mm
Blockage length ( $L_b$ )	-	100 mm	100 mm
Wall thickness	0.57 mm	0.86 mm	1.38 mm

Up- and downstream Part II, we installed optical accesses for the PDA (Phase-Doppler Analyzer) and 3cLIF (Three-color Laser Induced Fluorescence) measurements. While the PDA measures the droplets diameter and axial velocity (in the  $z$ -direction), the 3cLIF thermometry provides the droplets mean temperature. An IR (infrared) camera is used to measure the tube temperature at the external surface, although we consider uniform temperature in the radial direction because Biot number is less than 0.1 for all the tests. A detailed explanation of these techniques is available in Labergue *et al.* article [9]. Furthermore, in the present work, we estimate the heat transfer dissipated by the internal flow with the following equation:

$$\varphi_{int}(z, t) = - \left( \frac{S_t \rho_w c_{p,w}}{\pi D_h} \right) \frac{dT_w(z, t)}{dt} - \left( \frac{D_{ext}}{D_h} \right) \varphi_l(z, t) \quad (2)$$

where  $\varphi_{int}$  is the heat flux (that is a function of the axial position  $z$  and the time  $t$ ),  $\rho_w$  and  $C_{p,w}$  are, respectively, the density and the specific heat of the tube material,  $T_w$  is the tube temperature measured by the IR camera,  $D_{ext}$  is the tube external diameter, and  $\varphi_l$  is the heat flux dissipation to the ambient by natural convection and radiation. The heat loss is estimated using the Stefan-Boltzmann equation for the radiative heat transfer and a vertical plate correlation for the convection [10].

The droplets generated downstream of Part II is preheated before injection to approximate their state to saturation, which is typical during a LOCA. The mass flow rate is 2 kg/h and their diameter after injection is approximately 500  $\mu\text{m}$ ; however, breakup occurs in the steam-droplets mixer and we have a polydispersed distribution in size at the inlet of Part II. Regarding the steam injection line, up to 10 kg/h of water vapor at saturation is generated in the boiler and then superheated at about 200  $^{\circ}\text{C}$  before mixing with the droplets. Naturally, the steam is slightly cooled down before reaching Part II.

The test procedure is the following (Figure 3):

1. First, we start the steam injection line to preheat the components of the experimental apparatus.
2. Afterward, we start the droplet injection so we have the internal two-phase flow and we start and adjust the DC power supply to set the temperature of Part II between 600  $^{\circ}\text{C}$  and 800  $^{\circ}\text{C}$ .
3. At this moment, we measure the droplets diameter and velocity upstream of Part II with the PDA, then we measure the droplets mean temperature up- and downstream of Part II with the 3cLIF thermometry.
4. The DC power supply is turned off so we start the cooling of the vertical pipe with the internal two-phase flow. During this period, the droplets size and velocity are measured with the PDA downstream of Part II and, simultaneously, the temperature of the tube with the IR camera, both at 50 Hz acquisition rate of sampling.
5. The test is finished 60 s after the beginning of the cooling phase. All the collected data are treated with MatLab 2017b.

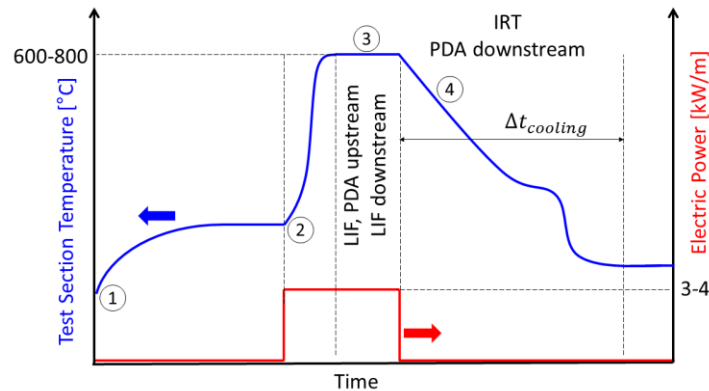


**Figure 3. Test procedure. (1) Start of the steam flow; (2) Start of the droplets injection and heating of the test section; (3) Measurement of the droplets characteristics; and (4) Cooling experiment.**

### 3. RESULTS AND DISCUSSION

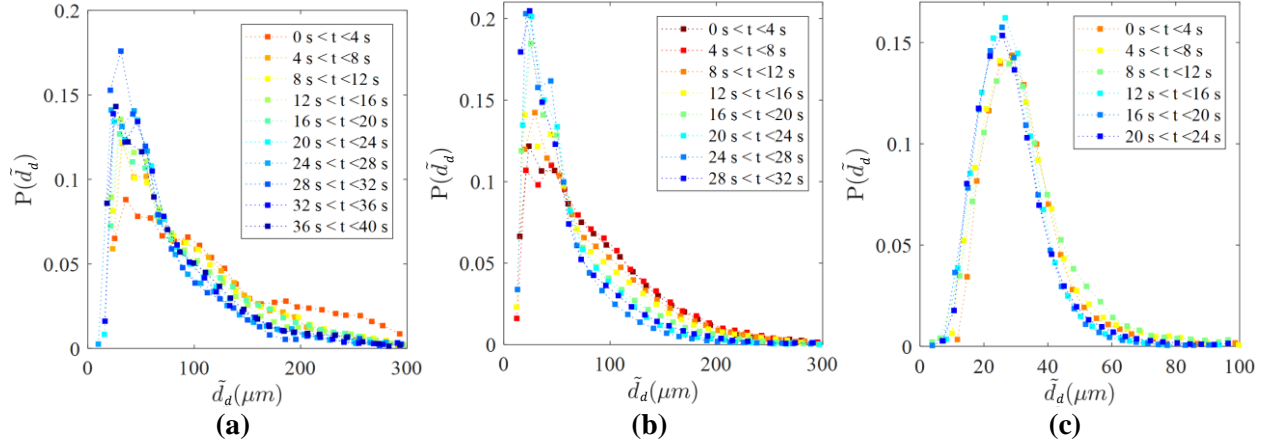
This section presents the results in the following order: flow conditions upstream of Part II, droplets characteristics downstream of Part II, and the internal heat dissipation during the cooling phase. For all the test cases, we fixed the values of 4.3 kg/h for the steam flow rate and of 0.8 kg/h for the liquid injection. Both the temperature of the steam and of the liquid before injection were similar for the three tests (170  $^{\circ}\text{C}$  and 63  $^{\circ}\text{C}$ , respectively).

Table II presents the droplets mean diameter and velocity upstream of Part II, where we can see similar conditions of the two-phase flow for all the test cases. This guarantees that the results we found during the cooling phase, which are presented in the next pages, reflect the effect of the geometry.

**Table II. Droplets characteristics upstream of Part II**

	<i>Configuration 1</i>	<i>Configuration 2</i>	<i>Configuration 3</i>
Droplets mean diameter	110 $\mu\text{m}$	88 $\mu\text{m}$	100 $\mu\text{m}$
Droplets mean velocity	16.0 m/s	14.5 m/s	12.5 m/s

We can see in Figure 4 the probability distribution  $P(\tilde{d}_d)$  of the droplets diameter  $\tilde{d}_d$  downstream of the heating tube for each test case and for different moments of the cooling phase. For the cases of 0% and 61% blockage ratios, the droplets diameter decreases with the time, which might be explained by the evaporation of the droplets and casual interactions between droplets and the heating wall that occurs more often at low wall temperatures. For the case of 90% blockage ratio, we observe a substantial decrease in the droplets diameter upstream of Part II. This happened because of the droplets breakup due to hydrodynamics instabilities caused by the large difference between velocities of the droplets and the steam at the restriction. Such phenomenon of droplets breakup was not observed with the 0% and 61% tubes. Hence, for these cases, we observed that droplets velocity  $\tilde{u}_d$  is lower for larger droplets, while it is almost constant for the 90% blockage ratio (Figure 5). However, for all the cases, we see a decrease in the droplets velocity in the course of the cooling phase because of the decrease in the steam velocity resulted by the decrease in the wall temperature and, hence, in the heat transfer from wall to vapor.



**Figure 4. Probability distribution of the droplets diameter downstream of Part II during the cooling phase for each configuration: (a) 0%, (b) 61% and (c) 90% blockage**

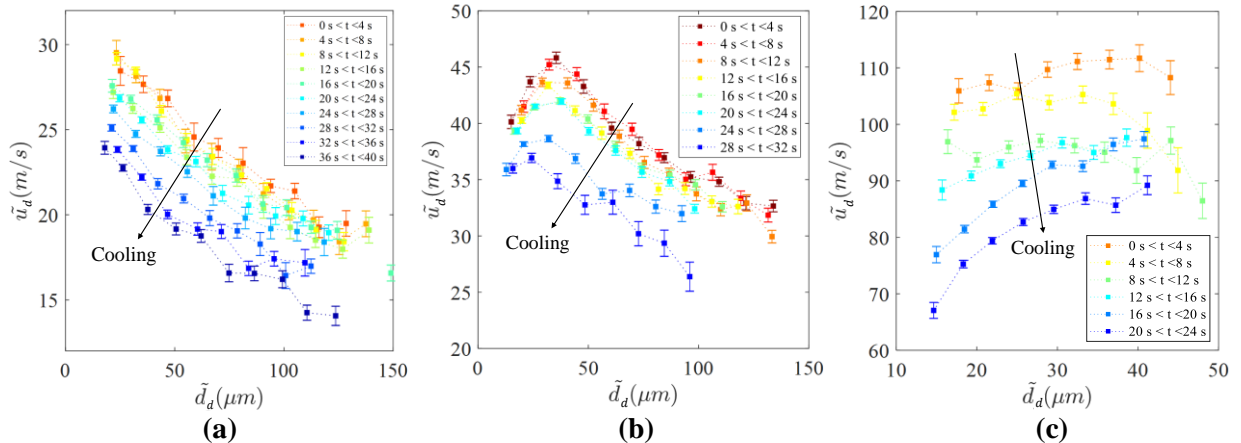


**Figure 5. Correlation of droplets diameter and velocity downstream of Part II during the cooling phase for each configuration: (a) 0%, (b) 61% and (c) 90% blockage**

Regarding the mean droplets temperature  $\bar{T}_d$  up- and downstream of Part II, Figure 6 presents the results of the 3cLIF measurements. We could not measure the downstream temperature with 90% blockage ratio because the droplets velocity is too high to be measured by the LIF acquisition system. The average temperature of the droplets upstream the heating tube is 85 °C, which means they were heated by the steam in the steam-droplets mixer (the liquid temperature before injection was 63 °C). However, the droplets temperature does not change after passing through the heated tube in Part II, if we consider the uncertainty of the measurement ( $\pm 5$  °C). Therefore, all the heat transfer between steam and droplet is directed to the droplets evaporation, i.e. latent heat.

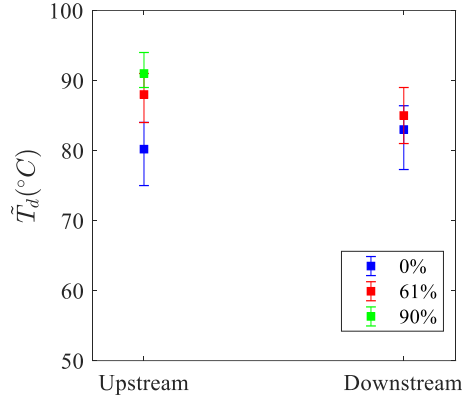


**Figure 6. Mean droplets temperature up- and downstream of Part II**

Finally, Figure 7 presents the variation in time and axial position of the heat dissipation by the internal two-phase flow in terms of rate of heat flow per unit length  $\Phi_{int}/L$ , calculated by:

$$\frac{\Phi_{int}}{L}(z, t) = \pi D_h \varphi_{int}(z, t) \quad (3)$$

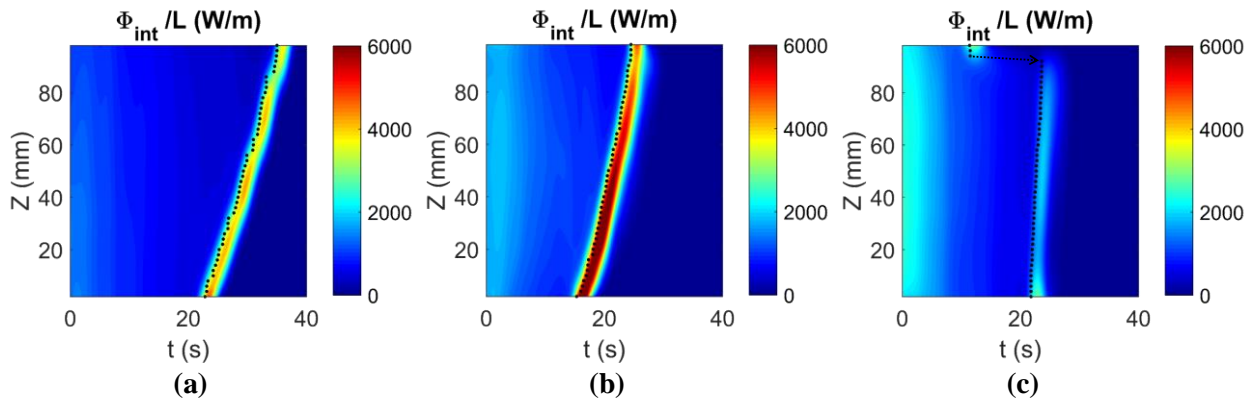


**Figure 7. Variation of the internal heat dissipation in time and axial position for each configuration: (a) 0%, (b) 61% and (c) 90% blockage ratio (dotted black line: rewetting front).**

We can see that the heat dissipation slowly decreases in time until rewetting occurs (represented by a dotted black line in the plots) and we observe a sudden increase in the heat flux. This happens because the droplets accomplish to impinge and wet the heating wall, change the heat transfer mechanism from film to nucleate boiling, where the heat transfer coefficients are much higher. Furthermore, in general, rewetting occurs from top to bottom and earlier with the increase in the blockage ratio. Especially for the

case of 90% blockage ratio, rewetting began at the top of the tube. This might have happened because of recirculation flow at the expansion of the tube after the restriction, which acts as a trap for the droplets that are no longer dragged by the flow and then fall onto the wall.

If we correlate the temperature and internal heat flux of each point from each map of Figure 7, we can plot a mean boiling curve as shown in Figure 8. In this plot, it is evident the higher heat dissipation with larger blockage ratios during the Leidenfrost regime because of the Venturi effect at the restriction that accelerates the steam flow. We can also see that the Leidenfrost temperature, the minimal point where rewetting occurs represented by the downward arrows in Figure 8, increases for 61% blockage ratio ( $T_{L,61\%} = 360\text{ }^{\circ}\text{C}$ ) compared with the 0% ( $T_{L,0\%} = 270\text{ }^{\circ}\text{C}$ ). This happens because the kinetic energy of droplets impinging the wall is higher with the 61% geometry, so they can wet the wall even at higher surface temperatures [11]. Because of the droplets breakup with the 90% blockage ratio mentioned before, the droplets kinetic energy decreases due to mass reduction and, consequently, the Leidenfrost temperature decreases again ( $T_{L,90\%} = 260\text{ }^{\circ}\text{C}$ ) comparing with the 61% blockage ratio.

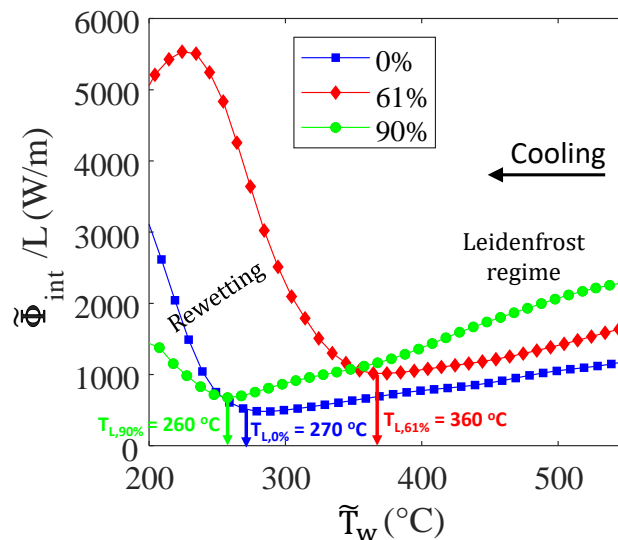


Figure 8. Mean boiling curves for each configuration, with the Leidenfrost temperature in evidence.

#### 4. CONCLUSIONS

In this experimental study, the effect of the blockage ratio on the cooling process of a vertical pipe with an internal steam-droplets flow is analyzed. The main findings are listed below:

- Droplets diameter and velocity decrease in the course of the cooling phase because of evaporation and reduction in the steam velocity.
- As expected, smaller droplets have higher velocity.
- With 90% blockage ratio, droplets breakup occurred because of hydrodynamic instabilities caused by the increase in the steam velocity at the restriction.
- Droplets mean temperature up- and downstream of Part II is practically the same, indicating that the heat transferred to the droplets is targeted to their evaporation.
- During the Leidenfrost regime, the higher the blockage ratio, the higher the heat dissipation by the imposed internal flow because of the Venturi effect.
- In general, wall rewetting occurs from bottom to top, increasing substantially the heat dissipation. Furthermore, the Leidenfrost temperature is highly dependent on the droplets kinetic energy.

It is important to remind that these experimental data and results must not be extrapolated to a situation of LOCA in a nuclear geometry. The present work is at sub-channel scale and, consequently, there is no bypass effect that changes significantly the effect of the blockage ratio.

## ACKNOWLEDGMENTS

This work is completed within the framework of RSNR Project PERFROI from a French State aid managed by the French National Research Agency under the program of Investments for the Future carrying the reference number ANR-11-RSNR-0017.

## REFERENCES

1. C. Grandjean, "Coolability of blocked regions in a rod bundle after ballooning under LOCA conditions. Main findings from a review of past experimental programmes." *Nucl. Eng. Des.* **237** (15–17 SPEC. ISS.), pp. 1872–1886 (2007).
2. G. Repetto, C. Dominguez, B. Durville, S. Carnemolla, D. Campello, C.N. Tardif, and M. Gradeck, "The R&D PERFROI project on thermal mechanical and thermal hydraulics behaviors of a fuel rod assembly during a loss of coolant accident." *Int. Top. Meet. Nucl. React. Therm. Hydraul. 2015, NURETH 2015.* pp. 1–14 (2015).
3. T. Glantz, T. Taurines, O. De Luze, S. Belon, G. Guillard, and F. Jacq, "DRACCAR: A multi-physics code for computational analysis of multi-rod ballooning, coolability and fuel relocation during LOCA transients Part one: General modeling description." *Nucl. Eng. Des.* **339** pp. 269–285 (2018).
4. T. Glantz, T. Taurines, S. Belon, O. De Luze, G. Guillard, and F. Jacq, "DRACCAR: A multi-physics code for computational analysis of multi-rod ballooning, coolability and fuel relocation during LOCA transients. Part Two: Overview of modeling capabilities for LOCA." *Nucl. Eng. Des.* **339** pp. 202–214 (2018).
5. K.H. Sun, J.M. Gonzales-Santalo, and C.L. Tien, "Calculation of Combined Radiation and Convection Heat Transfer in Rod Bundles Under Emergency Cooling Conditions." *J. Heat Transfer.* **98** (3), pp. 414–420 (1976).
6. Y. Guo and K. Mishima, "A non-equilibrium mechanistic heat transfer model for post-dryout dispersed flow regime." *Exp. Therm. Fluid Sci.* **26** (6–7), pp. 861–869 (2002).
7. M.J. Meholic, D.L. Aumiller, and F.B. Cheung, "A comprehensive, mechanistic heat transfer modeling package for dispersed flow film boiling - Part 2 - Implementation and assessment." *Nucl. Eng. Des.* **291** pp. 302–311 (2015).
8. J.D. Peña Carrillo, M. Gradeck, A. Labergue, and T. Glantz, "Identification of Heat Transfers for a Vapor-Droplets Flow Inside a Representative Fuel Assembly Subchannel - Experimental and Model Approach." *16th Int. Heat Transf. Conf.* pp. 1–8 (2018).
9. A. Labergue, J.D. Peña Carrillo, M. Gradeck, and F. Lemoine, "Combined three-color LIF-PDA measurements and infrared thermography applied to the study of the spray impingement on a heated surface above the Leidenfrost regime." *Int. J. Heat Mass Transf.* **104** pp. 1008–1021 (2017).
10. Y.A. Çengel and A.J. Ghajar, "Heat and Mass Transfer: Fundamentals and Applications." *McGraw-Hill Education*, 2015.
11. P. Dunand, G. Castanet, M. Gradeck, D. Maillet, and F. Lemoine, "Energy balance of droplets impinging onto a wall heated above the Leidenfrost temperature." *Int. J. Heat Fluid Flow.* **44** pp. 170–180 (2013).